

Award Accounts

The Chemical Society of Japan Award for Creative Work for 2002

Preparation, Characterization, and Reactivities of Highly Functional Titanium Oxide-Based Photocatalysts Able to Operate under UV–Visible Light Irradiation: Approaches in Realizing High Efficiency in the Use of Visible Light

Masakazu Anpo

Department of Applied Chemistry, Graduate School of Engineering, Osaka Prefecture University, 1-1, Gakuen-cho, Sakai, Osaka 599-8531

Received January 8, 2004; E-mail: anpo@ok.chem.osakafu-u.ac.jp

A review of the research advances made in the design and development of highly reactive and functional titanium oxide photocatalysts, which can utilize not only UV but also visible or solar light, and a clarification of the active sites as well as the detection of the reaction intermediates at the molecular level have been presented here. The potential for the effective utilization and conversion of solar energy into useful and safe chemical energy by the modification of the electronic properties of such TiO_2 photocatalysts is great when one considers their myriad applications as well as their non-polluting qualities. Such a modification process by methods such as ion-implantation can be applied not only for semiconducting bulk TiO_2 photocatalysts but also for TiO_2 thin film photocatalysts and titanium oxide photocatalysts highly dispersed within zeolite frameworks. Moreover, the photocatalytic reactivity of semiconducting TiO_2 nano-powders was found to be dramatically enhanced by the loading of small amounts of Pt. This worked to enhance the reduction reaction, resulting in the charge separation of the electrons and holes generated by light irradiation. In addition, highly dispersed titanium oxide species prepared within zeolite frameworks as well as SiO_2 or Al_2O_3 matrices showed much higher and unique photocatalytic performances as compared to semiconducting bulk TiO_2 photocatalysts. Significantly, a new alternative method to directly prepare such visible light-responsive TiO_2 thin film photocatalysts on various substrates has been successfully developed by applying a RF magnetron sputtering deposition method.

Environmental pollution and destruction on a global scale, as well as the lack of sufficient clean and natural energy sources have drawn much attention and concern to the vital need for ecologically clean chemical technology, materials, and processes—one of the most urgent challenges facing chemical scientists. Since the discovery of the photosensitization effect of the TiO_2 electrode on the electrolysis of water into H_2 and O_2 by Honda and Fujishima in 1972,[1] photocatalysis by TiO_2 semiconductors has been widely studied with the aim of efficiently converting light energy into reliable and effective chemical energy.[2–14] Especially significant are photocatalytic processes that can make use of clean, safe, and abundant solar energy. In this regard, TiO_2 semiconductor fine nano-particles are ideal and powerful photocatalysts due to their chemical stability, non-toxicity and high reactivity for the elimination of pollutants in air and water. UV light irradiation of TiO_2 semiconductor nano-particles excites the electrons from valence band to conduction band, leaving holes in the valence band. As shown in the primary processes (Scheme 1), when the TiO_2 photocatalystst is excited by UV light in the presence of O_2 and H_2O, which corresponds to an aqueous phase or atmospheric

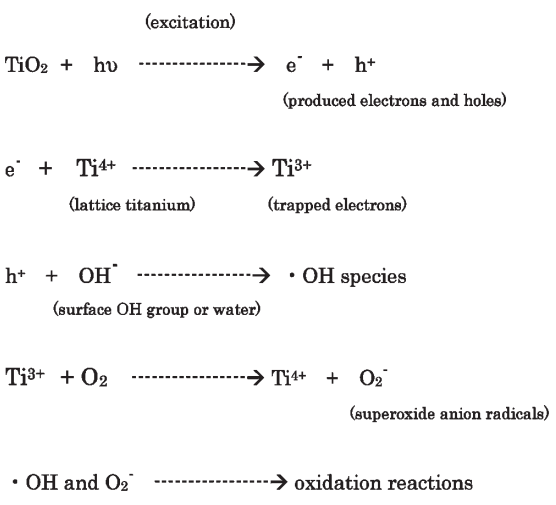

Scheme 1. Primary processes of the photocatalytic reaction on TiO_2 photocatalysts in the presence of H_2O and O_2.

Published on the web August 6, 2004; DOI 10.1246/bcsj.77.1427

environment, the photo-formed electrons and holes generate active oxygen species such as O_2^- and $^\bullet OH$ radicals, respectively. These species can then initiate redox reactions with organic molecules adsorbed on the surface of the catalysts. Thus, TiO_2 photocatalysts exhibit the potential to oxidize a wide range of organic materials, including chlorinated organic compounds such as dioxins, into harmless compounds as CO_2 and H_2O. If solar energy can be applied, such systems would be effective even for dilute concentrations of toxic reactants in the atmosphere and water on a huge global scale.[15–25]

For the preparation of such well-defined photocatalytic systems, it is important to identify and clarify the chemical features for the formation of the electrons and holes, their charge separation and migration to the surface sites where the catalytic reactions proceed. It is also important to detect the reaction intermediate species and their dynamics, and to elucidate the reaction mechanisms at the molecular level. These tasks in turn necessitate detailed and comprehensive investigations into the relationship between the chemical nature of the photogenerated active sites and the local structures of the photocatalysts.[26–43]

Along these lines, detailed studies into the characterization of TiO_2 semiconductor nano-particles and various TiO_2-based various photocatalytic molecular systems using a number of molecular spectroscopies have been carried out. Two main objectives are sought: (i) the improvement of the photocatalytic reactivity and its efficiency,[44–111] and (ii) the design and development of TiO_2 photocatalysts which are able to absorb and work not only under UV but also visible or solar light irradiation.[112–157]

Investigations on semiconducting TiO_2 nano-particle photocatalysts showed that photocatalytic reactions could be remarkably enhanced by the addition of small amounts of a noble metal such as Pt. Such an enhancement in the photocatalytic reactivity has been explained in terms of a photoelectrochemical mechanism in which the electrons generated by UV light irradiation of the TiO_2 semiconductors quickly transfered to the Pt particles loaded onto the TiO_2 surface where the reduction reactions proceeded. As a result, these Pt particles worked to effectively enhance the charge separation of the photo-formed electrons and holes, leading to a marked improvement in the photocatalytic performance. Time-resolved spectroscopic investigations and ESR measurements clearly indicated the important roles of these Pt particles in the dynamics of such photo-formed charge carriers and in the reaction sites.[108–111]

Studies have also been carried out on extremely small size TiO_2 nano-particles as well as on various binary oxides including extremely small size TiO_2 moieties, such as TiO_2/SiO_2, TiO_2/Al_2O_3, and TiO_2/B_2O_3.[65,67,70–79] In particular, we have found that semiconducting TiO_2 nano-sized particles of less than 100 Å show significant enhancement in photocatalytic reactivity attributed to the quantum size effect.[67,72–76] This phenomenon is due to an electronic modification of the TiO_2 photocatalysts as well as the close existence of the photo-formed electron and hole pairs. Their efficient contribution to the reaction from a different mechanism results in enhanced performance as compared to large-size TiO_2 bulk photocatalysts. These findings have provided us with new insights into such highly dispersed molecular-size titanium oxide photocatalysts on various supports. Moreover, the application of an anchoring method enables the preparation of molecular and/or cluster-sized photocatalysts on various supports such as SiO_2 and porous glasses. Highly dispersed titanium oxide species incorporated within the cavities or framework of zeolites were also investigated for their unique local structures, such as their 4-fold coordinated titanium oxide species and their efficient photocatalytic properties as compared to those of semiconducting large-size TiO_2 bulk powdered photocatalysts.

As an approach in the development of visible-light responsive catalysts, various photosensitizing dyes adsorbed and/or supported on semiconducting catalysts were investigated.[44–59] In these systems, the dyes absorb visible light to form electronically excited states. From these excited states, electrons are injected into the conduction band of the semiconducting catalyst, producing photosensitized photocatalysts which are able to work even under visible light irradiation. However, these photosensitizing dyes are not thermally and photochemically stable. Although numerous investigations have been carried out into visible light-responsive photocatalysts by adding small amounts of components such as cations and metal oxides, no significant results could be obtained and these initial trials were found to have limitations.[60–64] However, an advanced metal ion-implantation method was applied to modify the electronic properties of such TiO_2 photocatalysts by bombarding them with high energy metal ions. Thus it was discovered that implantation with various transition metal ions such as V, Cr, Fe, Co, and Ni by high voltage acceleration in the range of 50–200 keV could enable a large shift in the absorption band of these photocatalysts toward visible light regions, with differing levels of effectiveness. Such a large shift allowed the metal ion-implanted TiO_2 photocatalysts to effectively and efficiently absorb solar light of up to 25–35%.[23–27] Furthermore, during the preparation of TiO_2 thin-film photocatalysts using various ion-engineering techniques such as an ion cluster beam method, a completely new technique, an RF-magnetron sputtering deposition method, was also discovered to modify the TiO_2 thin-film photocatalysts so that they could absorb and operate even under visible light irradiation. With this method, it was found that the photocatalytic reactivity of these TiO_2 thin-films and the wavelength regions of the absorption of visible light greatly depended on the sputtering conditions, such as the pressure of the Ar sputtering gas and the substrate temperature. This most recent investigation is significant in that effective visible light-responsive TiO_2 thin-film photocatalysts could be developed at low cost with the RF-magnetron sputtering deposition method, in contrast to the high cost of using the advanced ion-implantation method.

Figures 1–3 show the advances made in the research of titanium oxide photocatalysts, which have led to breakthroughs for many practical applications. In the present account, the progress made in the development of effective TiO_2 photocatalysts will be reviewed in three chapters: (i) The design of highly efficient TiO_2 semiconductor photocatalysts; (ii) The design of highly dispersed titanium oxide photocatalysts and; (iii) The development of "second-generation TiO_2 photocatalysts" which can operate under visible light.

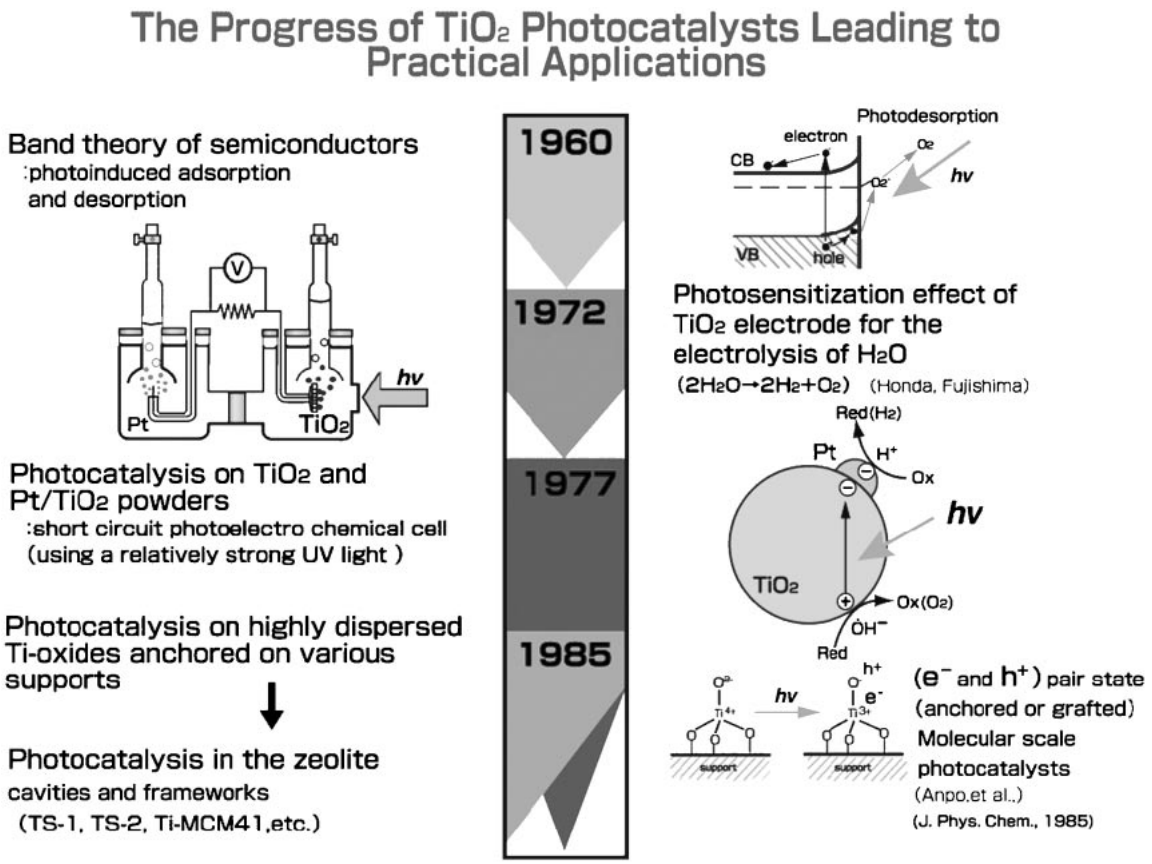

Fig. 1. The progress of the researches on TiO_2 photocatalysts leading to practical applications.

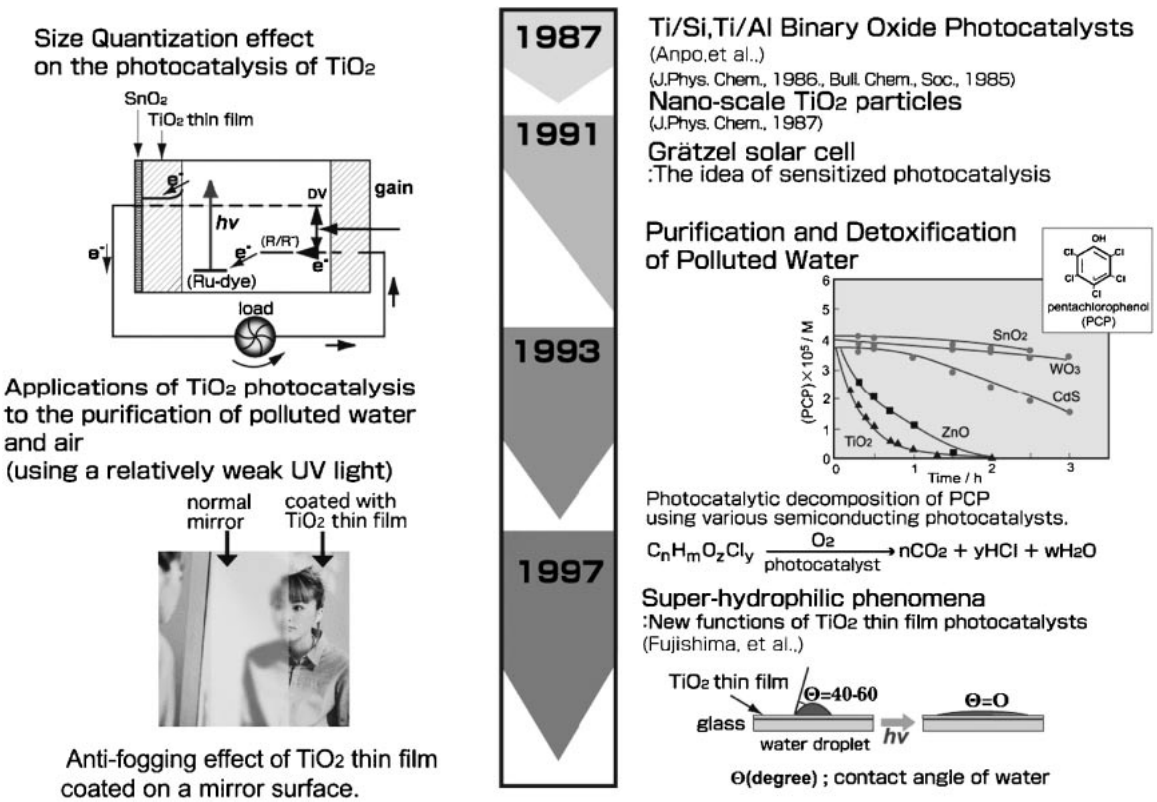

Fig. 2. The progress of the researches on TiO_2 photocatalysts leading to practical applications.

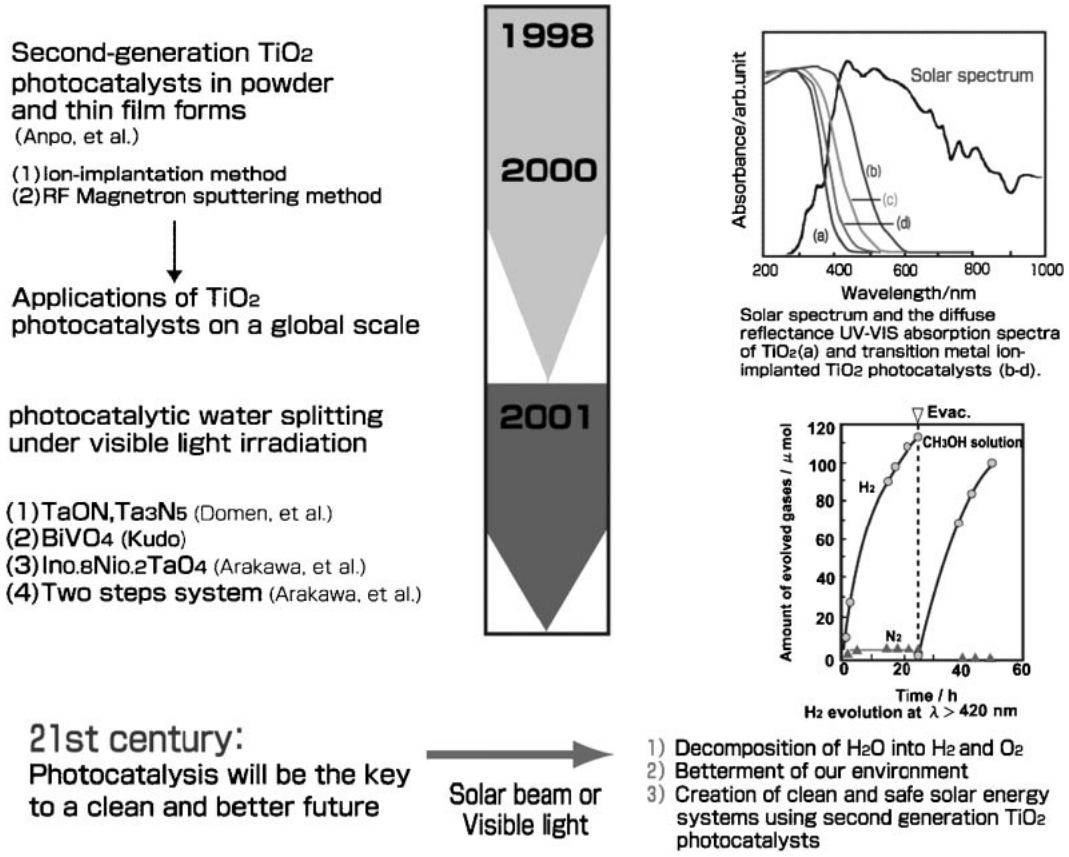

Fig. 3. The progress of the researches on TiO_2 photocatalysts leading to practical applications.

1. Design of Highly Efficient TiO_2 Semiconductor Photocatalysts

1.1 Pt Loading on Semiconducting TiO_2 Photocatalysts.[65–72,108–111] The photocatalytic reactivity of semiconducting TiO_2 is remarkably enhanced by the addition of small amounts of noble metals such as Pt or Rh. This effect can be explained by the quick transfer of photo-generated electrons in TiO_2 semiconductors to the loaded metal particles, resulting in efficient charge separation and a decrease in the electron and hole recombination. Although many studies have been carried out, there have been few direct investigations clarifying the metal loading effects on the primary processes involved in photocatalytic reactions in solid–gas systems.

UV light irradiation of the TiO_2 photocatalysts in the presence of sufficient amounts of water forming a monolayer of water on the wet TiO_2 surface with the coexistence of unsaturated hydrocarbons such as alkenes and alkynes led to the formation of alkanes by a hydrogenation reaction accompanied by the fission of the carbon–carbon bond of the reactant molecules (hereafter referred to as photo-hydrogenolysis). Alkanes formed without the fission of such a carbon–carbon bond (hereafter referred to as photohydrogenation) were observed as minor products. In addition to the formation of these saturated hydrocarbons, the formation of oxygen-containing compounds such as CH_3CHO, CO, and CO_2 could also be detected.[65,66,72]

Changes in the product yields depended on the amount of water remaining on the TiO_2 surface and also on the water pressure. Moreover, D-atom containing products in the photocatalytic hydrogenation reaction of unsaturated hydrocarbons with D_2O instead of H_2O could be observed. It could, therefore, be concluded that the non-dissociated water molecules adsorbed on the TiO_2 surface, and not the surface hydroxy groups, play an important role in the photocatalytic hydrogenolysis reaction.[66,69] The Pt-loaded TiO_2 photocatalyst was found to mainly catalyze the hydrogenation to form C_3H_8 without the carbon–carbon bond fission, while the unloaded TiO_2 photocatalyst was found to mainly catalyze the hydrogenolysis and lead to the formation of C_2H_6 and CH_4.

The growth of the ESR signals attributed to Ti^{3+} were observed both on Pt-loaded TiO_2 and unloaded TiO_2 photocatalysts under UV light irradiation. The signal intensity of Ti^{3+} for the unloaded TiO_2 was found to increase linearly with the UV light irradiation time, while few changes in the signal intensity could be observed with Pt-loaded TiO_2. The Ti^{3+} site was seen to arise from the Ti^{4+} site at which the photo-generated electrons were trapped. These results clearly indicate that photo-generated electrons in the Pt-loaded TiO_2 quickly transfer from TiO_2 to Pt particles, so that few Ti^{3+} sites could be observed. These electrons trapped on the Pt particles worked to enhance the reduction of the protons to form atomic hydrogens ($H^+ + e^- \rightarrow H$), leading to the hydrogenation reaction. As a result, the photocatalytic hydrogenation reaction was seen to be enhanced specifically by Pt loading. From these findings, the following mechanisms behind the observed photocatalytic reactions on unloaded TiO_2 and Pt-loaded TiO_2 catalysts could be proposed:

(i) In the case of unloaded TiO_2 photocatalysts, UV light irra-

diation of the TiO_2 catalysts generates electron and hole pairs that can be represented as localized electrons (Ti^{3+}) and holes, i.e., O^- (lattice) and/or $^{\bullet}OH$ radicals. Some of these electron and hole pairs disappeared by the recombination process on the bulk TiO_2, while other electrons and holes diffused to the surface of the TiO_2 catalysts to react with various hydrocarbons, which led to photocatalytic reactions such as hydrogenolysis and the formation of oxygen-containing organic compounds.[65,66,69,72,79,81]

(ii) In the case of Pt-loaded TiO_2 photocatalysts, the photo-generated electrons quickly transfered from TiO_2 to Pt particles and the holes remained on the TiO_2, resulting in a charge separation of the photo-formed electron and hole pairs with a good efficiency. As a result, the reduction reaction by the photo-formed electrons on the Pt particles and the oxidation reaction by the photo-formed holes on TiO_2 could both proceed, leading to photoelectrochemical reactions such as hydrogenation and oxidation. It could be seen that, in TiO_2 photocatalysts having rather large particle sizes, these photoelectrochemical reactions are predominant and are accompanied by a decrease in the contribution of the photocatalytic reactions.

Time-resolved spectroscopic experiments of these photocatalytic systems provide us more direct and detailed information on the dynamics of the photo-formed charge carriers, charge separation and/or recombination and charge transfer processes with high time resolution. For example, the transient absorption spectra of the Ti^{3+} species generated by the electron trapping were observed, they yielding an absorption band at around 500–650 nm and the temporal profile of its absorption for TiO_2 (P-25) excited by a femto-second laser pulse (390 nm) in a vacuum, respectively.[104–111]

As shown in Fig. 4, the electronic properties as well as the photocatalytic reactivity of titanium oxide photocatalysts dramatically change, depending on their structures, from an extended-semiconducting structure to nano-sized, extremely small particles, and molecular-sized titanium oxide species. Therefore, a detailed understanding of the relationship between the structure of the active surface sites and their reactivity at the molecular level is requisite for developing highly efficient and effective photocatalysts, as shown in Fig. 5.

1.2 Quantum Size Effect on Nano-Sized Photocatalysts.[72] Table 1 shows the results of the photocatalytic hydrogenation reaction of propyne (C_3H_4) with H_2O on rutile type TiO_2 catalysts having different particle sizes, together with the BET surface areas, wavelengths at the adsorption edge positions as well as the degree of the blue shift of the band gap compared with that of the bulk TiO_2 catalyst. As shown in Table 1, for both rutile and anatase type TiO_2 photocatalysts, the degree of the blue shifts in the absorption increased as the particle size of the catalysts decreased. In particular, for TiO_2 photocatalysts with a particle size of less than 100 Å, a large shift to shorter wavelength regions was observed for both catalysts, resulting in an increase in the quantum yields, though the BET surface area increased in a uniform manner when the particle size of the catalysts decreased.[72]

As already mentioned above, Pt-loaded TiO_2 photocatalysts were found to catalyze the photocatalytic hydrogenation reaction of C_3H_4 with H_2O to form hydrogenation products (i.e., C_3H_8) without the carbon–carbon bond fission. On the other hand, unloaded TiO_2 photocatalysts catalyzed the hydrogenolysis reaction to produce mainly CH_4, C_2H_6, and oxygen-containing products. Improvements in the quantum yield of the photocatalytic reactions with decreased particle diameters were also observed in the case of Pt-loaded TiO_2 photocatalysts. The results obtained from both unloaded and Pt-loaded TiO_2 were closely associated with the size quantization effect rather than with their physical properties such as their surface areas, resulting in a significant modification of the energy level in the local-

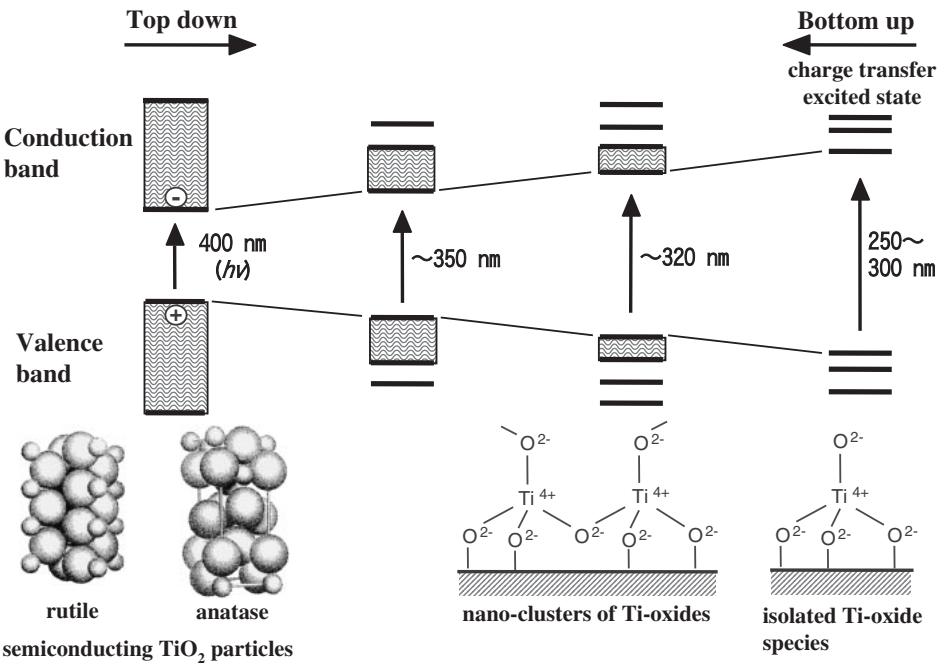

Fig. 4. The progress of the titanium oxide photocatalysts from extended semiconductoing TiO_2 particles, nano-scale molecular clusters, and then to the isolated Ti-oxide molecular species as well as the changes in their electronic states.

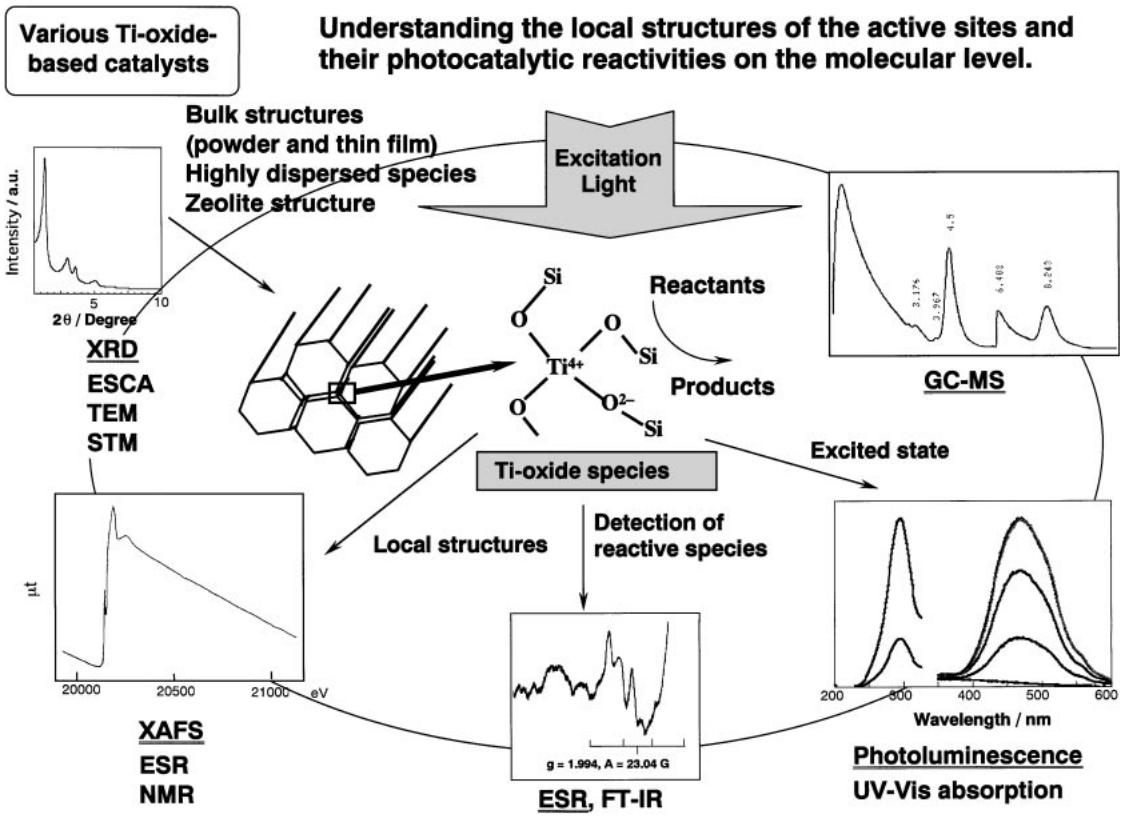

Fig. 5. Schematic description for the understanding of the relationship between the local structures of the active surface sites and their photocatalytic reactivity at the molecular level.

Table 1. Effect of Pt Loading on the Photocatalytic Hydrogenation of Propyne (C_3H_4) with H_2O on Rutile-Type TiO_2 Catalysts Having Various Particle Sizes

TiO_2 particle size /Å	BET surface area /$m^2\,g^{-1}$	Wavelength at band gap position /nm	Magnitude of the shift at band gap /eV	Pt content /wt %	Photohydrogenation products /10^{-8} mol g-cat h^{-1}			Selectivity (C_3H_8/C_2H_6)
					CH_4	C_2H_6	C_3H_8	
55	533	398	0.0934	0.0	60.2	290.0	1.1	0.0039
				4.0	28.9	160.0	1540.1	9.6
120	121	401.5	0.067	0.0	9.1	42.2	0.16	0.0038
				4.0	0.62	5.4	135.0	25.0
400	26	409.2	0.01	0.0	6.82	28.9	0.09	0.0032
				4.0	trace	1.0	56.0	56.0
2000	4.0	410.4	0.000	0.0	1.9	10.2	0.04	0.0039
				4.0	trace	0.24	23.8	99.0

Reaction carried out at 300 K.

ized photo-excited state of the TiO_2 photocatalysts. In other words, as the particle size of the photocatalysts decreased, the ratio of the surface to bulk increased. As a result, the photo-generated electron and hole pairs can easily and quickly diffuse to the surface of the catalysts to form the active sites at which the photocatalytic (redox) reactions are induced.

2. Design of Highly Dispersed Titanium Oxide Photocatalysts

2.1 Highly Dispersed Titanium Oxide Species Anchored onto Various Supports.[68–74] The results obtained from nano-sized fine particle TiO_2 photocatalysts were useful in the development of a well-defined and highly dispersed titanium oxide species supported or anchored on inert supports. The photocatalytic reactivities of highly dispersed titanium oxide species anchored onto such supports as porous glass, silica, and zeolites are interesting, since highly dispersed metal oxides can lead to dramatic modifications in their electronic and reactive properties, resulting in an enhancement of their photocatalytic reactivity and selectivity.

Titanium oxides anchored onto silica glass by the chemical vapor deposition (CVD) method exhibited an intense pre-edge peak in the XANES region. The presence of such a sharp pre-edge peak clearly indicates that the titanium oxide species on

the supports have a unique local structure in tetrahedral coordination. ESR is also a powerful technique in investigating the local structure of the titanium oxide species anchored onto supports. After photoreduction of the catalysts having a highly dispersed titanium oxide species with H_2 at 77 K, an ESR signal attributed to the tetrahedrally coordinated Ti^{3+} ions could be observed. These results were in good agreement with the those obtained from XAFS measurements.[70,74]

The titanium oxide species anchored onto silica glass also exhibited photoluminescence having a peak position at around 480 nm, when it was excited by UV light irradiation of around 260 nm. Only photocatalysts which exhibited a sharp pre-edge peak in the XANES spectra showed photoluminescence spectra at 77 K. From these results, it could be seen that the absorption and photoluminescence spectra of the highly dispersed titanium oxide species should be attributed to the following charge transfer process and to its reverse recombination process of the correlated electron-hole pairs, respectively.

$$(Ti^{4+}–O^{2-}) \rightleftarrows (Ti^{3+}–O^{-})^*. \quad (1)$$

The addition of O_2 or NO molecules led to the efficient quenching of the photoluminescence. The photoluminescence as well as its efficient quenching with the addition of O_2 or N_2O clearly indicate that the emitting sites, as the active sites, are highly dispersed on the support surface due to efficient interactions with these quencher molecules.

UV light irradiation of the anchored photocatalysts in the presence of unsaturated hydrocarbon and water was found to produce mainly hydrogenolysis products. The yield of the photocatalytic hydrogenolysis of C_3H_4 with H_2O was found to be in good agreement with the intensity of the photoluminescence spectra, indicating that of the charge transfer excited state, i.e., $(Ti^{3+}–O^{-})^*$, plays an important role in the photocatalytic hydrogenolysis on such highly dispersed titanium oxide catalysts. The initial reaction rate over these anchored titanium oxide photocatalysts was determined to be about 2–3 orders of magnitude higher than that of powdered TiO_2 photocatalysts.[68]

2.2 Photocatalytic Reactivity of Titanium Oxide Species Incorporated within Zeolite Frameworks.[112–127] It has been seen that highly dispersed titanium oxide species in 4-fold coordination anchored onto supports showed much higher and unique photocatalytic performance as compared to powdered TiO_2 catalysts. These highly dispersed species can also be prepared within zeolite frameworks in tetrahedral coordination.

The highly dispersed molecular-sized titanium oxide species incorporated within zeolite frameworks have been found to show unique photocatalytic performance, especially for the decomposition reaction of NO into N_2 and O_2[112–115] as well as the reduction of CO_2 with H_2O to form CH_3OH and CH_4.[110–121] UV light irradiation of these catalysts in the presence of NO at 275 K was found to lead to the effective decomposition of NO to produce N_2 and O_2 with a high selectivity, while the powdered bulk TiO_2 photocatalysts were found to decompose NO and mainly produce N_2O. Such highly dispersed molecular-sized titanium oxide species prepared within the zeolite framework also showed a remarkable enhancement in the selectivity for N_2 formation in the decomposition of NO as well as much higher reactivity as compared to semiconducting TiO_2 or the titanium oxide photocatalysts prepared by an impregnation method on silica and zeolite surfaces.[87–92,115,120–127]

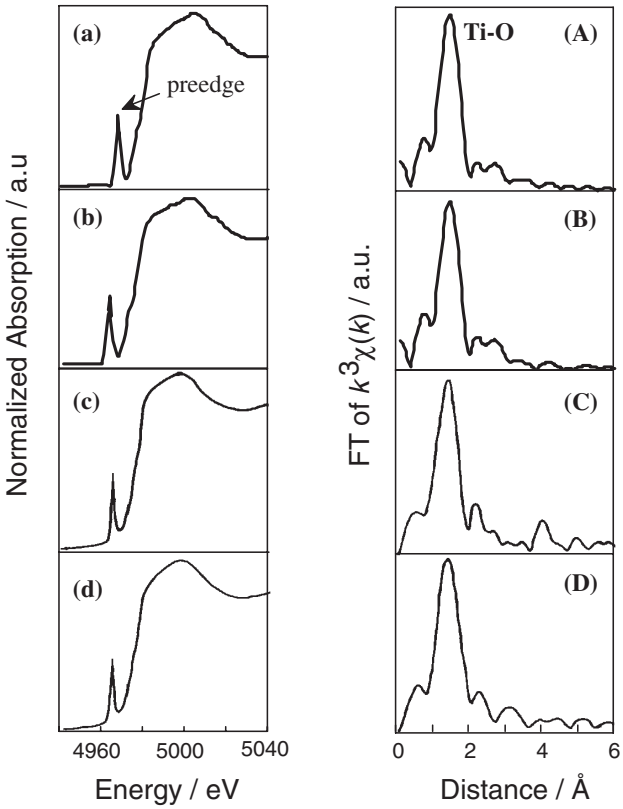

Fig. 6. Ti K-edge XANES (a–d) and Fourier transforms of EXAFS (A–D) spectra of the titanium oxide species incorporated within various zeolite frameworks. (a, A) Ti-beta (OH), (b, B) Ti-beta (F), (c, C) Ti/HMS, (d, D) Ti/MCM-41.

Figure 6 shows that the Ti K-edge XANES (left) and the Fourier transforms of EXAFS (right) of titanium oxides prepared within zeolite frameworks exhibit an intense pre-edge peak in the XANES region. The curve-fitting analysis of EXAFS oscillation clearly indicate that these catalysts consisted of 4-fold coordinated Ti ions and involved only a well-defined and isolated tetrahedral titanium oxide species having a Ti–O bond distance of about 1.83 Å. On the other hand, catalysts prepared by an impregnation method were found to contain an aggregated octahedral TiO_2 species.

In Fig. 7, these highly dispersed tetrahedral titanium oxide species incorporated within zeolite frameworks are shown to exhibit an efficient photoluminescence at around 490 nm by excitation at around 250 nm. These results clearly indicate the presence of a highly dispersed tetrahedrally coordinated titanium oxide species. Moreover, the photoluminescence spectrum attributed to the 4-fold coordinated titanium oxide species could be smoothly quenched by the addition of NO molecules, its extent depending on the amount of NO added. These findings indicate that the tetrahedrally coordinated titanium oxide species work as active sites accessible to the added NO and, furthermore, the added NO easily interacts with the charge transfer excited state, i.e., the $(Ti^{3+}–O^{-})^*$ electron-hole pairs of the tetrahedral titanium oxide species. Thus, the following reaction mechanism of the photocatalytic decomposition of

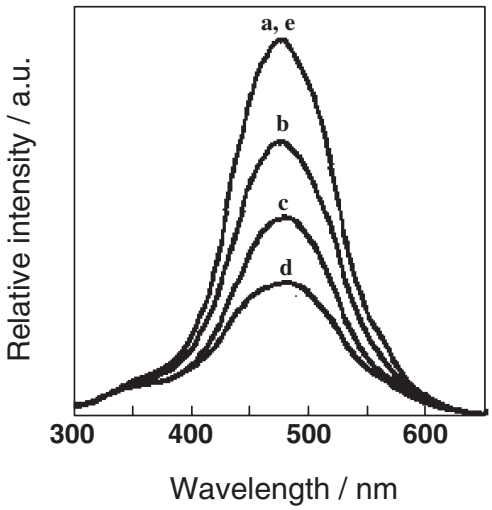

Fig. 7. The photoluminescence spectrum of the TS-2 catalyst at 77 K (a), and the effect of the addition of NO (b–d). NO pressure in Torr: (a) 0; (b) 0.05; (c) 0.1; (d) 0.3; (e) evacuation at 295 K after (d).

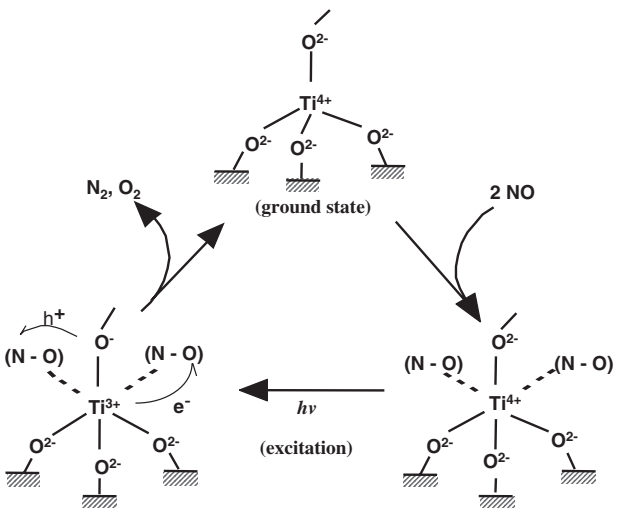

Chart 1. The reaction mechanism of the photocatalytic decomposition of NO into N_2 and O_2 on tetrahedrally coordinated Ti-oxide species under UV light irradiation.[112]

NO over the highly dispersed titanium oxide species has been proposed: the electron transfer from the Ti^{3+} site, at which the photo-formed electrons are trapped, into the anti-π^*-bonding orbital of NO takes place while the simultaneous electron transfer from the π-bonding orbital of NO into the O^- site, at which the photo-formed holes are trapped, occurs. Such a simultaneous electron transfer could lead to the direct decomposition of NO into N_2 and O_2 on tetrahedrally coordinated titanium oxide photocatalysts (Chart 1).[112]

2.3 Photocatalytic Reactivity of the Titanium Oxide-Based Binary Catalysts.[65–83] Titanium oxide-based binary catalysts combined with Al_2O_3 or SiO_2 can be easily prepared by the sol–gel or a precipitation method.[65–83] The X-ray diffraction patterns of these binary-type oxides decreased in intensity and also broadened in peak width when the Ti content was decreased. These results indicate that the crystalline size of the titanium oxide particles becomes smaller as the Ti content decreases. XAFS measurements of Ti/Si binary oxides having differing Ti content revealed that the binary oxides with lower Ti content (<10 wt %) contain a tetrahedral TiO_4 unit with a Ti–O bond distance of about 1.83 Å within the SiO_2 matrices, while binary oxides having higher Ti content (>50 wt %) consisted mainly of aggregated TiO_2 fine nano-particles.

With Ti/Si binary oxide catalysts, a characteristic photoluminescence was observed at a wavelength of 490 nm upon excitation by UV light of around 260 nm. This absorption and photoluminescence could be attributed to the charge transfer process and its reverse radiative deactivation from the excited state of the titanium oxide species, respectively. The peak positions of the photoluminescence were also observed to shift slightly toward shorter wavelength regions as the Ti content of the catalysts decreased; these results were in good agreement with the blue shifts in the absorption spectra.

These titanium oxide-based binary catalysts were found to show efficient photocatalytic reactivity and selectivity for various significant photocatalytic reactions, such as the hydrogenolysis reaction of unsaturated hydrocarbons with water, the decomposition of NO into N_2 and O_2, and the reduction of CO_2 with H_2O, as well as the oxidation of organic compounds in water. When the Ti content of these catalysts decreased, the selectivity for N_2 formation in the photocatalytic decomposition of NO increased. A good relationship between the intensity of photoluminescence and the yield of the photocatalytic reaction was also observed. Thus, the efficient photoluminescence of the highly dispersed 4-coordinated titanium oxide species indicated the important role that it plays in the photocatalytic decomposition of NO into N_2 and O_2 with high reactivity and selectivity.

2.4 The Photocatalytic Reduction of CO_2 with H_2O Using Titanium Oxide Incorporated within Zeolites (Ti/Zeolites).[116–132] The development of efficient photocatalytic systems which are able to reduce CO_2 with H_2O into chemically useful compounds such as CH_3OH or CH_4 are challenging goals in the research aimed at establishing environmentally-friendly catalysts. To meet this challenge, the development of highly dispersed tetrahedrally coordinated titanium oxide species within zeolite frameworks has been promising because of its high and unique photocatalytic reactivity for the reduction of CO_2 with H_2O, especially as compared with conventional bulk semiconducting TiO_2 catalysts.

Titanium oxides incorporated within various zeolite frameworks were seen to contain isolated 4-fold coordinated titanium oxide species having a Ti–O bond distance of about 1.83 Å. These Ti containing zeolite catalysts exhibited a photoluminescence spectrum at around 480–490 nm by excitation at around 220–260 nm. The addition of H_2O or CO_2 molecules onto the Ti/zeolite catalysts led to an efficient quenching of the photoluminescence as well as a shortening of the lifetime of the charge transfer excited state, its extent depending on the amount of the gasses added. Such an efficient quenching of the photoluminescence with H_2O or CO_2 molecules suggests not only that 4-fold coordinated titanium oxide species locate at positions accessible to these small molecules but that they also interact with these titanium oxides in both their ground and excited states. In fact, UV irradiation of the Ti/zeolite catalysts

in the presence of a mixture of CO_2 and H_2O led to the photocatalytic reduction of CO_2 to form CH_3OH and CH_4 as major products, as well as CO, O_2, C_2H_4, and C_2H_6 as minor products, in the gas phase at 323 K, while the yields of these photo-formed products increased with a good linearity against the UV irradiation time. These results clearly indicate that highly dispersed tetrahedrally coordinated titanium oxide species exhibit higher selectivity as well as better efficiency for CH_3OH formation in the photocatalytic reduction of CO_2 with H_2O, as compared with bulk TiO_2 in octahedral coordination.[116–132]

Figure 8 shows the relationship between the coordination number of the titanium oxide species of the Ti/zeolite catalysts obtained from XAFS analyses and the selectivity for the formation of CH_3OH in the photocatalytic reduction of CO_2 with H_2O on various Ti/zeolite catalysts. A clear dependence of the selectivity on the coordination numbers of the titanium oxide species could be observed, i.e., the lower the coordination number of the titanium oxide species, the higher the selectivity for CH_3OH formation. In contrast, bulk TiO_2 semiconducting photocatalysts did not show any reactivity for the formation of CH_3OH from CO_2 and H_2O. From these results, researchers could propose that the highly efficient and selective photocatalytic reduction of CO_2 with H_2O into CH_3OH can be achieved using Ti/zeolite catalysts involving highly dispersed 4-fold coordinated titanium oxides in their frameworks as the active species. In fact, the quantum yields for the formation of (CH_4 and CH_3OH) in the photocatalytic reduction of CO_2 with H_2O on transparent Ti-containing mesoporous silica thin-film zeolite was much high as to be 0.28% in comparison with 0.005% on bulk semiconducting TiO_2 particles. The selectivity for the formation of CH_3OH was also high to be about 30% on Ti-MCM-41 and 60% on Ti-containing mesoporous silica thin-film zeolite, respectively.

There are no limits to the possibilities and applications of photocatalytic systems for the purification of polluted air and water as well as the safe conversion of solar light energy into safe chemical energy. However, TiO_2 semiconductors have a relatively large band gap of 3.2 eV, corresponding to wavelengths shorter than 388 nm. In other words, TiO_2 in itself can make use of only 3–4% of the solar energy that reaches the earth, necessitating the use of a UV light source for its effective use as a photocatalyst. From this viewpoint, TiO_2 photocatalysts which would be able to operate efficiently under both UV and visible light irradiation would be ideal for practical and widespread use.[23–27]

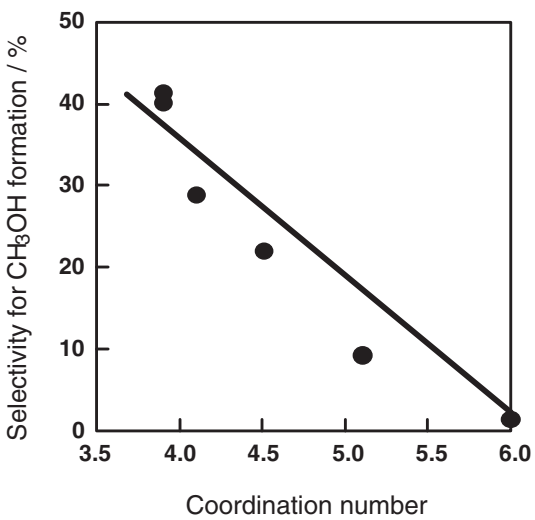

Fig. 8. The relationship between the coordination number of the titanium oxide species of the Ti/zeolite catalysts and the selectivity for the formation of CH_3OH in the photocatalytic reduction of CO_2 with H_2O on various Ti/zeolite catalysts.

3. Design and Development of "Second-Generation TiO_2 Photocatalysts" Which Can Operate under Visible Light Irradiation[133–157]

3.1 Modification of the Electronic State of TiO_2 by Applying an Advanced Metal Ion-Implantation Method.[133–155] A highly advanced metal ion-implantation method was applied to modify the electronic properties of bulk TiO_2 photocatalysts by bombarding them with high energy metal ions. It was discovered that such implantation with various transition metal ions, such as V, Cr, Mn, Fe, and Ni, accelerated by high voltage enabled a large shift in the absorption band of the titanium oxide catalysts towards the visible light region, with differing levels of effectiveness. However, Ar, Mg, or Ti ion-implanted TiO_2 exhibited no shift in the absorption spectra, showing that such a shift is not caused by the high-energy implantation process itself but by some interactions between the transition metal ions and the TiO_2 catalyst. The absorption band of the Cr ion-implanted TiO_2 shifts smoothly towards the visible light region, the extent of the red shift depending on the amount and type of metal ions implanted, with the absorption maximum and minimum values always remaining constant, as can be seen in Fig. 9(b–d). The order of effectiveness in the red shift was found to be as follows: V > Cr > Mn > Fe > Ni ions. Such a shift allows the metal ion-implanted titanium oxide to use solar irradiation more effectively, with efficiencies in the range of 20–30%.

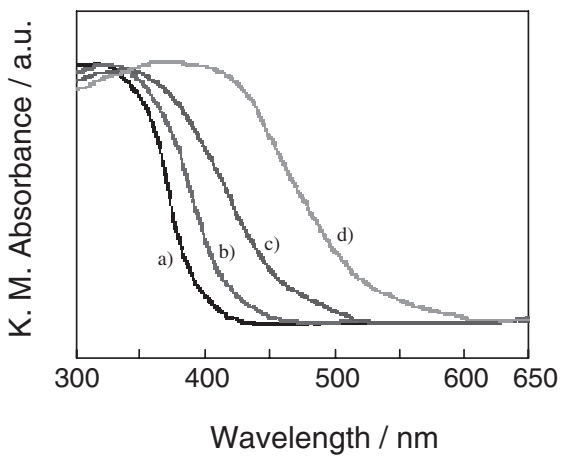

Fig. 9. The UV–vis absorption spectra of TiO_2 (a) and Cr ion-implanted TiO_2 photocatalysts (b–d). The amount of implanted Cr ions (μmol/g): (a) 0; (b) 0.22; (c) 0.66; (d) 1.3.

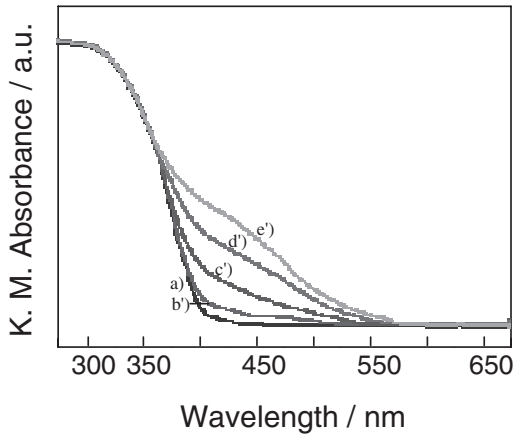

Fig. 10. The UV–vis absorption spectra of TiO_2 (a) and Cr ion-doped TiO_2 (b′–d′) photocatalysts prepared by an impregnation method. The amount of doped Cr ions (wt %): (a) 0; (b′) 0.01; (c′) 0.1; (d′) 0.5; (e′) 1 (0.1 wt % equals 4.9 μmol/g-TiO_2).

Furthermore, such red shifts in the absorption band of the metal ion-implanted TiO_2 catalysts were observed for any kind of titanium oxide except the amorphous types, the extent of the shift differing from sample to sample. It was also found that such shifts in the absorption band could be observed only after calcination of the metal ion-implanted TiO_2 samples in O_2 at around 723–823 K. Therefore, it is clear that calcination under O_2 atmosphere in combination with metal ion-implantation was instrumental in the red shift of the absorption spectrum toward visible light regions. These results clearly show that such shifts in the absorption band of the TiO_2 catalysts by metal ion-implantation are a general phenomenon and not a special feature of certain kinds of bulk TiO_2 catalysts.

Figure 10 shows the absorption spectra of the TiO_2 catalysts impregnated or chemically doped with Cr ions in large amounts as compared with those for the Cr ion-implanted samples. The Cr ion-doped catalysts showed no shift in the absorption edge of TiO_2; however, a new absorption band appears at around 420 nm as a shoulder peak due to the formation of the impurity energy level within the band gap, its intensity increasing with the amounts of Cr ions chemically doped. These results indicate that the method of doping causes the electronic properties of the TiO_2 catalyst to be modified in completely different ways, thus confirming that only metal ion-implanted TiO_2 catalysts show such shifts in the absorption band toward visible light regions, even with much lower amounts of the ions, as compared with those for the chemically doped systems.

Neither with the unimplanted original TiO_2 nor with the chemically doped TiO_2 catalysts does the photocatalytic reaction proceed under visible light irradiation ($\lambda > 450$ nm). However, visible light irradiation of such advanced metal ion-implanted TiO_2 catalysts enabled them to initiate various significant photocatalytic reactions. Visible light irradiation ($\lambda > 450$ nm) of the Cr ion-implanted TiO_2 catalysts in the presence of NO at 275 K led to the decomposition of NO into N_2, O_2, and N_2O with a good linearity against the light irradiation time. Under the same conditions of visible light irradiation, the unimplanted original pure TiO_2 catalyst did not exhibit any photocatalytic reactivity. Moreover, the action spectrum for this reaction on the metal ion-implanted TiO_2 was in good agreement with the absorption spectrum of the catalyst shown in Fig. 9, indicating that only metal ion-implanted TiO_2 catalysts were effective for the photocatalytic decomposition reaction of NO under visible light irradiation. Thus, it was found that metal ion-implanted TiO_2 catalysts could absorb visible light up to a wavelength of 400–600 nm and could thus operate effectively as photocatalysts: hence the name, "second-generation TiO_2 photocatalysts".[133–154]

It is important to emphasize that the photocatalytic reactivity of the metal ion-implanted TiO_2 catalysts retained the same photocatalytic efficiency as the unimplanted original TiO_2 catalyst under UV light irradiation ($\lambda < 380$ nm). When metal ions were chemically doped into the TiO_2 catalyst, the photocatalytic efficiency decreased dramatically even under UV irradiation; this was due to the quick recombination of the photoformed electrons and holes through the impurity energy levels formed by the doped metal ions within the band gap of the catalyst (Fig. 10). These results clearly show that metal ions that are physically implanted do not work as electron and hole recombination centers, but work only to modify the electronic properties of the catalyst.

Various fieldwork experiments were conducted to test the photocatalytic reactivity of the newly developed TiO_2 catalysts under solar beam irradiation.[153] Under outdoor solar light at ordinary temperatures, the Cr and V ion-implanted TiO_2 catalysts showed several times higher photocatalytic reactivity for the decomposition of NO than the unimplanted original TiO_2 catalysts. It was also found the V ion-implanted TiO_2 catalysts showed several times higher photocatalytic reactivity for the hydrogenation of C_3H_4 with H_2O than the original TiO_2. These results, together with the results shown in Fig. 9, clearly indicate that, by using second-generation titanium oxide photocatalysts developed by applying the metal ion-implantation method, the effective and efficient use of visible and solar light energy by photocatalysis is now possible.

The relationship between the depth profiles of the metal ions implanted within TiO_2 having the same amounts of metal ions, such as V or Cr ions, and their photocatalytic efficiency under visible light irradiation was investigated. It was found that, when the same amounts of metal ions were implanted into the deep bulk of the TiO_2 catalyst by applying high acceleration energy, the catalyst exhibited high photocatalytic efficiency under visible light irradiation. On the other hand, when low acceleration energy was applied, the catalyst exhibited low photocatalytic efficiency under the same conditions of visible light irradiation.

Increasing the number (or amounts) of metal ions implanted into the deep bulk of the TiO_2 catalyst was found to cause the photocatalytic efficiency to increase under visible light irradiation, passing through a maximum at around 6×10^{16} ions/cm^2, then decreasing with a further increase in the number of metal ions implanted. The presence of ions at the near surfaces could be observed by ESCA measurements only on samples implanted with a large amount of metal ions. These results clearly show that there are optimal conditions in the depth and amount of metal ions implanted to achieve high photocatalytic reactivity under visible light irradiation.

The ESR spectra of the V ion-implanted TiO_2 catalysts were measured before and after calcination of the samples in O_2 at around 723–823 K. Distinct and characteristic reticular V^{4+} ions were detected only after calcination at around 723–823 K. When a shift in the absorption band towards visible light regions by the V ion-implantation was observed, the presence of the reticular V^{4+} ions could be detected by ESR measurements. No such V ions having the same local structure or shifts in the absorption band could be observed with TiO_2 catalysts chemically doped with V ions.

The XANES and Fourier transforms of the EXAFS oscillations for the TiO_2 catalysts chemically doped and also physically implanted with Cr ions were measured in order to clarify the local structures of these Cr ions. Results obtained from the analyses of the XAFS spectra showed that, for the TiO_2 catalysts chemically doped with Cr ions by an impregnation or sol–gel method, the ions were present as aggregated Cr-oxides in octahedral coordination similar to Cr_2O_3 and in tetrahedral coordination similar to CrO_3, respectively. On the other hand, in the catalysts physically implanted with Cr, the ions were found to be present in a highly dispersed and isolated state in octahedral coordination, clearly suggesting that the Cr ions are incorporated in the lattice positions of the TiO_2 catalyst in place of the Ti ions.[133–154]

These findings clearly show that the success in modifying the electronic state of TiO_2 by metal ion-implantation, enabling the absorption of visible light even longer than 550 nm, is closely associated with the strong and long-distance interaction which arises between the TiO_2 and the metal ions implanted, and not by the formation of impurity energy levels within the band gap of the catalysts. While the impurity energy levels are appeared due to the formation of aggregated metal oxide clusters, which are often observed in the chemical doping of metal ions and/or oxides, as shown in Fig. 10.

These results obtained in the photocatalytic reactions and various spectroscopic measurements of the catalysts clearly indicate that the implanted metal ions are highly dispersed within the deep bulk of the TiO_2 catalysts and work to modify the electronic nature of the catalysts without any changes in the chemical properties of the surfaces. These modifications were found to be closely associated with an improvement in the reactivity and sensitivity of the TiO_2 photocatalyst, thus enabling the TiO_2 catalyst to absorb and operate effectively not only under UV but also under visible light irradiation. As a result, under outdoor solar light irradiation at ordinary temperatures, transition metal ion-implanted TiO_2 catalysts showed several times higher photocatalytic efficiency than the unimplanted original TiO_2 catalysts.

3.2 Visible Light Responsive Ti-Oxide/Zeolites.[112–128,142–149] The XANES spectra of Ti/zeolite at the Ti K-edge clearly showed intense pre-edge peaks, which are related to the local structures surrounding the titanium oxide species in tetrahedral symmetry.[112–128] The Fourier transforms of the EXAFS spectra for these Ti/zeolite catalysts exhibited a strong peak at around 1.83 Å, which could be assigned to the neighboring oxygen atoms, i.e., a Ti–O bond, indicating the presence of an isolated titanium oxide species. Moreover, curve-fitting analysis of the Fourier transforms for the EXAFS spectra showed that the titanium oxide species incorporated within the zeolite frameworks exist in tetrahedral coordination with a Ti–O bond distance of about 1.83 Å for various Ti/zeolite catalysts.[142–149]

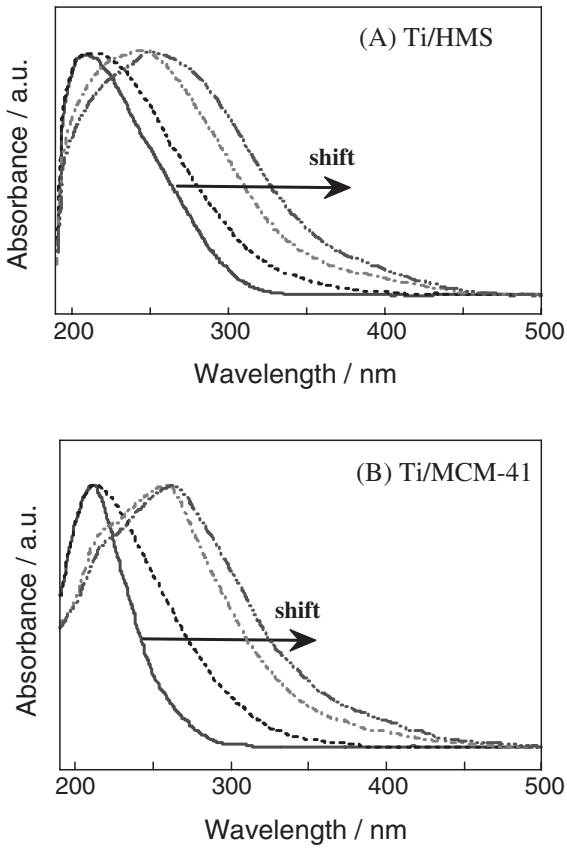

Fig. 11. The diffuse reflectance UV–vis absorption spectra of the V ion-implanted Ti/HMS (A) and Ti/MCM-41 (B). The amount of implanted V ions (μmol/g-cat): (a) 0; (b) 0.66; (c) 1.3; (d) 2.0.

Figure 11 shows the diffuse reflectance UV–vis absorption spectra of the V ion-implanted Ti/HMS and Ti/MCM-41 catalysts. The absorption spectra of these catalysts at around 200–260 nm can be attributed to the charge transfer absorption process involving an electron transfer from the O^{2-} to Ti^{4+} ions of the highly dispersed tetrahedrally coordinated TiO_4 unit of these catalysts. These absorption spectra shift smoothly towards visible light regions, the extent strongly depending on the amount of V ions implanted. These results clearly suggest that the interaction of the implanted V ions with the TiO_4 units leads to the modification of the electronic properties of the titanium oxide species within the zeolite frameworks.

The V K-edge FT-EXAFS spectra of the Ti/HMS catalyst implanted with V ions indicate that the next-neighbours of the V environment are not the same as vanadium oxide based catalysts (e.g., V_2O_5) and suggests the formation of tetrahedral titanium oxides having a V–O–Ti bond instead of V–O–V linkages. These findings for the V–O–Ti bridge structures in the V ion-implanted Ti/HMS and also in the Ti/MCM-41 catalysts support the findings shown by the red shift in the absorption spectra for these catalysts.

The photocatalytic reactivity of the V ion-implanted Ti/HMS and Ti/MCM-41 (and Ti/zeolite catalysts such as Ti-beta

zeolite) catalysts for the decomposition of NO into N_2 and O_2 under visible light irradiation ($\lambda > 420$ nm) has been investigated. UV irradiation ($\lambda < 300$ nm) of Ti/HMS, Ti/MCM-41, and other Ti/zeolite catalysts in the presence of NO led to an efficient decomposition of NO into N_2 and O_2. However, as expected from their absorption spectra, the unimplanted original Ti/HMS, Ti/MCM-41, and other Ti/zeolites did not work to catalyze the photocatalytic decomposition of NO under visible light irradiation. Moreover, visible light irradiation of the V ion-implanted Ti/HMS, Ti/MCM-41, and other Ti/zeolite catalysts led to the efficient decomposition of NO into N_2 and O_2, and the yield of the photo-formed N_2 increased linearly with the irradiation time. These results clearly indicate that this decomposition reaction proceeds on the V ion-implanted Ti/HMS, Ti/MCM-41, and other Ti/zeolite catalysts under both UV and visible light irradiation.[56] It was also confirmed that NO decomposition does not proceed at all under UV ($\lambda < 300$ nm) nor under visible light irradiation ($\lambda > 420$ nm) on the V ion-implanted HMS, MCM-41, and other zeolites. Also, the titanium oxide species in the Ti/zeolite, Ti/HMS, and Ti/MCM-41 catalysts were shown to be present in tetrahedral coordination within the zeolite frameworks. The implanted V ions and the highly dispersed Ti-oxide species form the Ti–O–V linkage, which leads to the modification of the electronic properties of the tetrahedral Ti-oxide species. These new properties enable the absorption of visible light to initiate reactions ($\lambda > 420$ nm) with high photocatalytic efficiency for the decomposition of NO into N_2 and O_2.[58–60]

3.3 Application of a RF Magnetron Sputtering Deposition Method to Design TiO_2 Thin-Film Photocatalysts Which Operate under Visible Light Irradiation.[155–157] A radio-frequency magnetron (RF-MS) deposition method has recently been developed to prepare TiO_2 thin-film photocatalysts, using a TiO_2 plate as the sputtering target and Ar as the sputtering gas. Thus, an alternative and more practical method to prepare transparent TiO_2 thin-films which can initiate various significant photocatalytic reactions effectively even under visible light irradiation could be successfully realized.[155–157] Figure 12 shows the UV–vis absorption transmittance spectra of the TiO_2 thin-films prepared by the RF-MS deposition method at different substrate temperatures. The thin-films prepared at relatively low temperatures ($T < 473$ K) exhibit high transparency and clear specific interference fringes in the visible light region, indicating that highly transparent and uniform thin-films have been formed on the substrate. The thin-films prepared at relatively high temperatures ($T > 773$ K) exhibit an efficient absorption in the visible light region, having a maximum absorption with the thin-film prepared at 873 K. In fact, these TiO_2 thin-films exhibited photocatalytic effectiveness for various reactions, such as the decomposition of NO as well as the oxidation of acetaldehyde with O_2, under both UV and visible light irradiation.

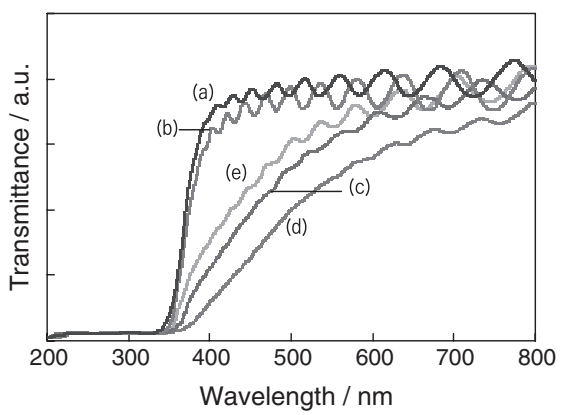

Fig. 12. The UV–vis absorption (transmittance) spectra of TiO_2 thin films prepared by a RF-MS deposition method. Preparation temperatures (K): (a) 373; (b) 473; (c) 673; (d) 873; (e) 973.

4. Conclusion

A summary of the preparation of nano-sized TiO_2 particles, highly dispersed titanium oxide species within zeolite cavities, titanium oxide based binary catalysts, and second-generation TiO_2 photocatalysts which can operate under visible light irradiation by an advanced metal ion-implantation method as well as by a new, more low-cost RF magnetron sputtering method has been presented. Detailed characterizations of these visible light-responsive TiO_2 thin-film photocatalysts were carried out at the molecular level, along with investigations into the various significant photocatalytic reactions that could be initiated.

The direct detection of the reaction intermediate species at the molecular level provided important information in explaining and clarifying the reaction mechanisms behind the observed photocatalytic reactions as well as the electronic properties of the photocatalyst surface. Furthermore, the advanced metal ion-implantation method and the RF-MS deposition method have opened the way to many innovative possibilities in the utilization of solar or visible light energy by realizing the development of unique second-generation TiO_2 photocatalysts and visible light-responsive molecular-sized titanium oxide species incorporated within the cavities and frameworks of zeolites and mesoporous molecular sieves. A combination of these fascinating and unique zeolite-incorporated systems and advanced ion-engineering techniques will provide new approaches in the utilization of solar energy as the most abundant and safe energy source, significantly to address environmental pollution on a large global scale as well as realizing the production of H_2 in the photocatalytic splitting of H_2O by solar irradiation.

The author thanks his colleagues (Drs. H. Yamashita, M. Matsuoka, and N. Zhanpeisov) and Ph.D students (Drs. N. Negishi, H. Nishiguchi, S. C. Moon, S. G. Zhang, Y. Ichihashi, M. Harada, S. Higashimoto, K. Ikeue, M. Takeuchi, S. W. Joo, Y. Shioya, and S. Dohshi) as well as many graduate-school students and post-graduate students for their cooperation, and he also thanks Profs. M. Che, S. Coluccia, E. Giamello, H. Patterson, and T. Fujii for their useful suggestions and comments throught the long international and domestic collaborations.

References

1 K. Honda and A. Fujishima, *Nature*, **238**, 37 (1972).

2 T. Inoue, A. Fujishima, S. Konishi, and K. Honda, *Nature*, **277**, 637 (1979).

3 T. Kawai and T. Sakata, *Chem. Phys. Lett.*, **72**, 87 (1980).
4 T. Kawai and T. Sakata, *Nature*, **286**, 31 (1980).
5 G. N. Schrauzer and A. J. Bard, *J. Am. Chem. Soc.*, **99**, 7189 (1977).
6 B. Kraeutler and A. J. Bard, *J. Am. Chem. Soc.*, **100**, 2239 (1978); *J. Am. Chem. Soc.*, **100**, 5985 (1978).
7 A. Heller, A. A. Shalom, W. A. Bonner, and B. Miller, *J. Am. Chem. Soc.*, **104**, 1688 (1982).
8 M. A. Fox, *Acc. Chem. Res.*, **16**, 314 (1983).
9 M. A. Fox and M. T. Dulay, *Chem. Rev.*, **93**, 341 (1993).
10 S. Sato and J. M. White, *J. Am. Chem. Soc.*, **102**, 7206 (1980).
11 H. Courbon, J. M. Herrmann, and P. Pichat, *J. Catal.*, **72**, 129 (1981).
12 M. Anpo and H. Yamashita, "Surface Photochemistry," ed by M. Anpo, Wiley, London (1996).
13 M. Anpo and H. Yamashita, "Heterogeneous Catalysis," ed by M. Schiavello, Wiley, London (1997).
14 M. Anpo, "Handbook of Heterogeneous Catalysis," ed by G. Ertl, H. Knozinger, and J. Weitkamp, Wiley-VCH, Weinheim (1997), and references therein.
15 L. P. Childs and D. F. Ollis, *J. Catal.*, **66**, 383 (1980).
16 A. L. Pruden and D. F. Ollis, *J. Catal.*, **82**, 404 (1983).
17 I. Ait-Ichou, M. Formenti, B. Pommier, and S. J. Teichner, *J. Catal.*, **91**, 193 (1985).
18 J. L. Falconer and K. A. Magrini-Bair, *J. Catal.*, **179**, 171 (1998).
19 M. C. Blount and J. L. Falconer, *J. Catal.*, **200**, 21 (2001).
20 T. Tatsuma, S. Tachibana, and A. Fujishima, *J. Phys. Chem. B*, **105**, 6987 (2001).
21 "Photocatalytic Purification and Treatment of Water and Air," ed by D. F. Ollis and H. Al-Ekabi, Elsevier, Amsterdam (1993).
22 "Photocatalysis—Fundamentals and Applications," ed by N. Serpone and E. Pelizzetti, Wiley, New York (1989).
23 M. Anpo, "Green Chemistry," Oxford University Press (2000), p. 1.
24 M. Anpo, *Pure Appl. Chem.*, **72**, 1265 (2000).
25 M. Anpo, *Stud. Surf. Sci. Catal.*, **130**, 157 (2000).
26 M. Anpo, "Photocatalysis," Kodansha Ltd., Tokyo and Springer-Verlag, Berlin (2002), p. 175.
27 M. Anpo, M. Takeuchi, H. Yamashita, S. Kishiguchi, A. Davidson, and M. Che, "Semiconductor Photochemistry and Photophysics," Marcel Dekker, Inc. (2003), p. 283.
28 G. Calzaferri, "Solar Energy Materials and Solar Cells, Proceedings of the 10th International Conference on Photochemical Transfer and Storage of Solar Energy," Elsevier (1995).
29 M. Anpo, "Surface Photochemistry," Wiley (1996).
30 Y. Kubokawa, K. Honda, and Y. Saito, "Hikarishokubai (Photocatalysis)," Asakura-shoten (1988).
31 M. Anpo, "Photofunctional Zeolites," ed by M. Anpo, NOVA Publishers Inc. (2000).
32 M. Anpo and S. Higashimoto, *Stud. Surf. Sci. Catal.*, **135**, 123 (2001).
33 A. Corma, *Chem. Rev.*, **97**, 2373 (1997).
34 T. Maschmeyer, F. Rey, G. Sankar, and J. M. Thomas, *Nature*, **378**, 159 (1995).
35 K. I. Zamaraev and J. M. Thomas, *Adv. Catal.*, **41**, 335 (1996).
36 S. Bordiga, S. Coluccia, C. Lamberti, L. Marchese, F. Boscherini, F. Buffa, F. Genoni, G. Leofanti, G. Petrini, and G. Vlaic, *J. Phys. Chem.*, **98**, 4125 (1994).
37 L. Marchese, T. Maschmeyer, E. Gianotti, S. Coluccia, and J. M. Thomas, *J. Phys. Chem. B*, **101**, 8836 (1997).
38 C. Lamberti, S. Bordiga, D. Arduino, A. Zecchina, F. Geobaldo, G. Spano, F. Genoni, G. Petrini, A. Carati, F. Villain, and G. Vlaic, *J. Phys. Chem. B*, **102**, 6382 (1998).
39 M. S. Rigutto and H. Van Bekkum, *Appl. Catal.*, **68**, 297 (1991).
40 G. Centi, S. Perathoner, F. Trifiró, A. Aboukais, C. F. Aïssi, and M. Guelton, *J. Phys. Chem.*, **96**, 2617 (1992).
41 S. Dzwigaj, M. Matsuoka, R. Franck, M. Anpo, and M. Che, *J. Phys. Chem. B*, **102**, 6309 (1998).
42 S. Dzwigaj, M. Matsuoka, M. Anpo, and M. Che, *J. Phys. Chem. B*, **104**, 6012 (2000).
43 H. Yamashita, K. Yoshizawa, M. Ariyuki, S. Higashimoto, M. Che, and M. Anpo, *Chem. Commun.*, **2001**, 435.
44 B. O'Regan and M. Gratzel, *Nature*, **353**, 737 (1991).
45 K. Kalyanasundaram and M. Gratzel, *Angew. Chem., Int. Ed. Engl.*, **18**, 701 (1979).
46 E. Borgarello, J. Kiwi, M. Gratzel, E. Pelizzetti, and M. Visca, *J. Am. Chem. Soc.*, **104**, 2996 (1982).
47 Y. Tachibana, J. E. Moser, M. Gratzel, D. R. Klug, and J. R. Durrant, *J. Phys. Chem.*, **100**, 20056 (1996).
48 W. D. K. Clark and N. Sutin, *J. Am. Chem. Soc.*, **99**, 4676 (1977).
49 P. V. Kamat and M. A. Fox, *Chem. Phys. Lett.*, **102**, 379 (1983).
50 K. R. Gopidas and P. V. Kamat, *J. Phys. Chem.*, **93**, 6428 (1989).
51 C. Nasr, K. Vinodgopal, S. Hotchandani, A. Chattopadhyaya, and P. V. Kamat, *J. Phys. Chem.*, **100**, 8436 (1996).
52 L. Ziolkowski, K. Vinodgopal, and P. V. Kamat, *Langumuir*, **13**, 3124 (1997).
53 K. Murakoshi, G. Kano, Y. Wada, S. Yanagida, H. Miyazaki, M. Matsumoto, and S. Murasawa, *J. Electroanal. Chem.*, **396**, 27 (1995).
54 K. Tennakone, G. R. R. A. Humara, A. R. Kumarasinghe, K. G. U. Wijayantha, and P. M. Sirimanne, *Semicond. Sci. Technol.*, **10**, 1689 (1995).
55 M. Gratzel, *J. Sol.-Gel Sci. Technol.*, **22**, 7 (2001).
56 K. Hara, H. Sugihara, Y. Tachibana, A. Islam, M. Yanagida, K. Sayama, H. Arakawa, G. Fujihashi, T. Horiguchi, and T. Kinoshita, *Langmuir*, **17**, 5992 (2001).
57 A. Islam, H. Sugihara, K. Hara, L. P. Singh, R. Katoh, M. Yanagoda, Y. Takahashi, S. Murata, and H. Arakawa, *J. Photochem. Photobiol., A*, **145**, 135 (2001).
58 K. Hara, H. Horiuchi, R. Katoh, L. P. Singh, H. Sugihara, K. Sayama, S. Murata, M. Tachiya, and H. Arakawa, *J. Phys. Chem. B*, **106**, 374 (2002).
59 K. Sayama, S. Tsukagoshi, K. Hara, T. Ohga, A. Shimpo, Y. Abe, S. Suga, and H. Arakawa, *J. Phys. Chem. B*, **106**, 1363 (2002).
60 A. K. Ghosh and H. P. Maruska, *J. Electrochem. Soc.*, **124**, 1516 (1977).
61 E. Borgarello, J. Kiwi, M. Gratzel, E. Pelizetti, and M. Visca, *J. Am. Chem. Soc.*, **104**, 2996 (1982).
62 M. R. Hoffman, S. T. Martin, W. Choi, and D. W. Bahnemann, *Chem. Rev.*, **95**, 69 (1995).
63 J. M. Jerrmann, J. Disdier, and P. Pichat, *Chem. Phys. Lett.*, **108**, 618 (1984).
64 H. P. Maruska and A. K. Ghosh, *Sol. Energy Mater.*, **1**, 237 (1979).

65 M. Anpo, N. Aikawa, S. Kodama, and Y. Kubokawa, *J. Phys. Chem.*, **84**, 569 (1984); C. Yun, M. Anpo, S. Kodama, and Y. Kubokawa, *J. Chem. Soc., Chem. Commun.*, **1980**, 609.
66 M. Anpo, N. Aikawa, and Y. Kubokawa, *J. Phys. Chem.*, **88**, 3998 (1984).
67 M. Anpo, T. Shima, and Y. Kubokawa, *Chem. Lett.*, **1985**, 1799.
68 M. Anpo, N. Aikawa, Y. Kubokawa, M. Che, C. Louis, and E. Giamello, *J. Phys. Chem.*, **89**, 5017 (1985).
69 M. Anpo and Y. Ichihashi, "Proceedings of the 15th International Congress on Catalysis, The Taniguchi Conference," Kobe (1995), p. 39.
70 S. Kodama, H. Nakaya, M. Anpo, and Y. Kubokawa, *Bull. Chem. Soc. Jpn.*, **58**, 3645 (1985).
71 M. Anpo, M. Yabuta, S. Kodama, and Y. Kubokawa, *Bull. Chem. Soc. Jpn.*, **59**, 259 (1986).
72 M. Anpo, T. Shima, S. Kodama, and Y. Kubokawa, *J. Phys. Chem.*, **91**, 4305 (1987).
73 M. Anpo and Y. Kubokawa, *Rev. Chem. Intermed.*, **8**, 105 (1987).
74 M. Anpo, H. Nakaya, S. Kodama, Y. Kubokawa, K. Domen, and T. Onishi, *J. Phys. Chem.*, **90**, 1633 (1988).
75 M. Anpo, T. Kawamura, S. Kodama, K. Maruya, and T. Onishi, *J. Phys. Chem.*, **92**, 438 (1988).
76 M. Anpo, T. Shima, and M. Che, *Chem. Express*, **3**, 403 (1988).
77 H. Yamashita, S. Kawasaki, Y. Ichihashi, M. Harada, M. Takeuchi, and M. Anpo, *J. Phys. Chem. B*, **102**, 5870 (1998).
78 H. Yamashita, S. Kawasaki, Y. Ichihashi, M. Takeuchi, M. Harada, and M. Anpo, *Korean J. Chem. Eng.*, **15**, 491 (1998).
79 M. Anpo, K. Chiba, M. A. Fox, and M. Che, *Bull. Chem. Soc. Jpn.*, **64**, 543 (1991).
80 S. Dohshi, M. Takeuchi, and M. Anpo, *J. Nanosci. Nonotechnol.*, **1**, 337 (2001).
81 M. Anpo, S. Dohshi, and M. Takeuchi, *J. Ceram. Process. Res.*, **3**, 258 (2002).
82 S. Dohshi, M. Takeuchi, and M. Anpo, *Catal. Today*, **85**, 199 (2003).
83 H. Yamashita, H. Nishiguchi, M. Anpo, and M. A. Fox, *Res. Chem. Intermed.*, **20**, 815 (1994).
84 M. Anpo, H. Yamashita, Y. Ichihashi, and S. Ehara, *J. Electroanal. Chem.*, **396**, 21 (1995).
85 H. Yamashita, Y. Ichihashi, M. Harada, G. Stewart, M. A. Fox, and M. Anpo, *J. Catal.*, **158**, 97 (1996).
86 M. Anpo, T. Shima, T. Fujii, and M. Che, *Chem. Lett.*, **1987**, 65.
87 G. Martra, S. Horokoshi, M. Anpo, S. Coluccia, and H. Hidaka, *Res. Chem. Intermed.*, **28**, 359 (2002).
88 M. Anpo and K. Chiba, *J. Mol. Catal.*, **74**, 207 (1992).
89 M. Anpo, M. Tomonari, and M. A. Fox, *J. Phys. Chem.*, **93**, 7300 (1989).
90 H. Yamashita, Y. Ichihashi, M. Anpo, M. Hashimoto, C. Louis, and M. Che, *J. Phys. Chem.*, **100**, 16041 (1996).
91 S. G. Zhang, Y. Ichihashi, H. Yamashita, T. Tatsumi, and M. Anpo, *Chem. Lett.*, **1996**, 895.
92 H. Yamashita and M. Anpo, *Surf. Sci. Jpn.*, **17**, 30 (1996).
93 M. Anpo, S. G. Zhang, and H. Yamashita, "Proceedings of the 11th International Congress on Catalysis," Baltimore (1996), p. 941.
94 M. Anpo, H. Yamashita, Y. Ichihashi, Y. Fujii, and M. Honda, *J. Phys. Chem. B*, **101**, 2632 (1997).
95 H. Yamashita, M. Honda, M. Harada, Y. Ichihashi, and M. Anpo, *J. Phys. Chem. B*, **102**, 10707 (1998).
96 A. Furube, T. Asahi, H. Masuhara, H. Yamashita, and M. Anpo, *J. Phys. Chem. B*, **103**, 3120 (1999).
97 D. R. Park, J. L. Zhang, K. Ikeue, H. Yamashita, and M. Anpo, *J. Catal.*, **185**, 114 (1999).
98 Y. Yoshida, M. Matsuoka, S.-C. Moon, H. Mametsuka, E. Suzuki, and M. Anpo, *Res. Chem. Intermed.*, **26**, 567 (2000).
99 H. Yamashita, M. Harada, A. Tanii, M. Honda, M. Takeuchi, Y. Ichihashi, and M. Anpo, *Stud. Surf. Sci. Catal.*, **130**, 1931 (2000).
100 S. Dohshi, M. Takeuchi, and M. Anpo, *J. Nanosci. Nanotechnol.*, **1**, 337 (2001).
101 H. Furube, T. Asahi, H. Masuhara, H. Yamashita, and M. Anpo, *Res. Chem. Intermed.*, **27**, 177 (2001).
102 H. Furube, T. Asahi, H. Masuhara, H. Yamashita, and M. Anpo, *Chem. Phys. Lett.*, **336**, 424 (2001).
103 M. Takeuchi, M. Matsuoka, H. Yamashita, and M. Anpo, *J. Synchrotron Rad.*, **8**, 643 (2001).
104 J. Zhang, Y. Hu, M. Matsuoka, H. Yamashita, M. Minagawa, H. Hidaka, and M. Anpo, *J. Phys. Chem. B*, **105**, 8395 (2001).
105 M. Ogawa, K. Ikeue, and M. Anpo, *Chem. Mater.*, **13**, 2900 (2001).
106 J. Zhang, M. Minagawa, M. Matsuoka, H. Yamashita, and M. Anpo, *Catal. Lett.*, **66**, 241 (2000).
107 J. Zhang, M. Minagawa, T. Ayusawa, S. Natarajan, H. Yamashita, M. Matsuoka, and M. Anpo, *J. Phys. Chem. B*, **104**, 11501 (2000).
108 A. Furube, T. Asahi, H. Masuhara, H. Yamashita, and M. Anpo, *Chem. Phys. Lett.*, **336**, 424 (2001).
109 A. Furube, T. Asahi, H. Masuhara, H. Yamashita, and M. Anpo, *Chem. Lett.*, **1997**, 735.
110 A. Furube, T. Asahi, H. Masuhara, H. Yamashita, and M. Anpo, *J. Phys. Chem. B*, **103**, 3120 (1999).
111 A. Furube, T. Asahi, H. Masuhara, H. Yamashita, and M. Anpo, *Res. Chem. Intermed.*, **27**, 1, 177 (2001).
112 M. Anpo, S. G. Zhang, S. Higashimoto, M. Matsuoka, H. Yamashita, Y. Ichihashi, Y. Matsumura, and Y. Souma, *J. Phys. Chem. B*, **103**, 9295 (1999).
113 S. G. Zhang, Y. Fujii, H. Yamashita, K. Koyano, T. Tatsumi, and M. Anpo, *Chem. Lett.*, **1997**, 659.
114 J. Zhang, M. Minagawa, M. Matsuoka, H. Yamashita, and M. Anpo, *Catal. Lett.*, **66**, 241 (2000).
115 J. Zhang, M. Matsuoka, H. Yamashita, and M. Anpo, *J. Synchrotron Rad.*, **8**, 637 (2001).
116 M. Anpo, T. Suzuki, E. Giamello, and M. Che, "New Developments in Selective Oxidation," Elsevier, Amsterdam (1990), p. 683.
117 M. Anpo, M. Kondo, S. Coluccia, C. Louis, and M. Che, *J. Am. Chem. Soc.*, **111**, 8791 (1989).
118 S. G. Zhang, M. Ariyuki, H. Mishima, S. Higashimoto, H. Yamashita, and M. Anpo, *Microporous Mesoporous Mater.*, **21**, 621 (1998).
119 S. G. Zhang, S. Higashimoto, H. Yamashita, and M. Anpo, *J. Phys. Chem. B*, **102**, 5590 (1998).
120 M. Anpo, H. Yamashita, Y. Fujii, Y. Ichihashi, S. G. Zhang, D. R. Park, S. Ehara, S. E. Park, J. S. Chang, and J. W. Yoo, *Stud. Surf. Sci. Catal.*, **114**, 177 (1998).
121 M. Anpo, H. Yamashita, K. Ikeue, Y. Fujii, S. G. Zhang, Y. Ichihashi, D. R. Park, Y. Suzuki, K. Koyano, and T. Tatsumi, *Catal. Today*, **44**, 327 (1998).
122 H. Yamashita, Y. Fujii, Y. Ichihashi, S. G. Zhang, K. Ikeue,

D. R. Park, K. Koyano, T. Tatsumi, and M. Anpo, *Catal. Today*, **45**, 221 (1998).
123 K. Ikeue, H. Yamashita, and M. Anpo, *Chem. Lett.*, **1999**, 1135.
124 K. Ikeue, H. Mukai, H. Yamashita, S. Inagaki, M. Matsuoka, and M. Anpo, *J. Synchrotron Rad.*, **8**, 640 (2001).
125 K. Ikeue, H. Yamashita, and M. Anpo, *J. Phys. Chem. B*, **105**, 8350 (2001).
126 K. Ikeue, H. Yamashita, T. Takewaki, M. E. Davis, and M. Anpo, *J. Synchrotron Rad.*, **8**, 602 (2001).
127 K. Ikeue, S. Nozaki, M. Ogawa, and M. Anpo, *Catal. Lett.*, **80**, 111 (2002).
128 M. Matsuoka and M. Anpo, *J. Photochem. Photobiol., C*, **3**, 225 (2003).
129 M. Anpo, M. Takeuchi, K. Ikeue, and S. Dohshi, *Curr. Opin. Solid State Mater. Sci.*, **6**, 381 (2002).
130 K. Ikeue, S. Nozaki, M. Ogawa, and M. Anpo, *Catal. Today*, **74**, 241 (2002).
131 H. Yamashita, K. Ikeue, T. Tatewaki, and M. Anpo, *Top. Catal.*, **18**, 95 (2002).
132 Y. Shioya, K. Ikeue, M. Ogawa, and M. Anpo, *Appl. Catal.*, in press (2004).
133 Y. Ichihashi, H. Yamashita, and M. Anpo, *Kinou-Zairyou (Functional Materials)*, **16**, 12 (1996).
134 M. Anpo, H. Yamashita, and Y. Ichihashi, *Optronics*, **186**, 161 (1997).
135 M. Anpo, *Catal. Surv. Jpn.*, **1**, 169 (1997).
136 M. Anpo, Y. Ichihashi, M. Takeuchi, and H. Yamashita, *Res. Chem. Intermed.*, **24**, 143 (1998).
137 M. Anpo, Y. Ichihashi, M. Takeuchi, and H. Yamashita, "Science and Technology in Catalysis 1998," ed by H. Hattori and K. Otsuka, Kodan-sha, Tokyo (1999), p. 305.
138 M. Anpo, M. Takeuchi, H. Yamashita, T. Hirao, N. Itoh, and N. Iwamoto, "Proceedings of the 4th International Conference ECOMATERIAL," Gifu (1999), p. 333.
139 M. Anpo and M. Che, *Adv. Catal.*, **44**, 119 (1999), and references therein.
140 M. Anpo, Y. Ichihashi, M. Takeuchi, and H. Yamashita, *Stud. Suf. Sci. Catal.*, **121**, 305 (1999), Proc. Tocat-3, Tokyo.
141 M. Anpo, M. Takeuchi, S. Kishiguchi, and H. Yamshita, *Surf. Sci. Jpn.*, **20**, 60 (1999).
142 M. Anpo, H. Yamashita, S. Kanai, K. Sato, and T. Fujimoto, U. S. Patent 6077492 (June 20, 2000).
143 M. Takeuchi, H. Yamashita, M. Matsuoka, T. Hirao, N. Itoh, N. Iwamoto, and M. Anpo, *Catal. Lett.*, **66**, 185 (2000).
144 M. Takeuchi, H. Yamashita, M. Matsuoka, T. Hirao, N. Itoh, N. Iwamoto, and M. Anpo, *Catal. Lett.*, **67**, 135 (2000).
145 M. Anpo, S. Dohshi, M. Kitano, and Y. Hu, "Metal Oxides: Chemistry and Applications," Marcel Dekker Inc. (2004), in press.
146 M. Anpo, *Pure Appl. Chem.*, **72**, 1265 (2000).
147 M. Anpo, *Stud. Surf. Sci. Catal.*, **130**, 157 (2000).
148 M. Anpo, S. Kishiguchi, Y. Ichihashi, M. Takeuchi, H. Yamashita, K. Ikeue, B. Morin, A. Davidson, and M. Che, *Res. Chem. Intermed.*, **27**, 45, 459 (2001).
149 M. Anpo, Keynote Lecture, "Studies in Surface Science and Catalysis," 130, in "12th International Congress on Catalysis," ed by A. Corma, F. V. Melo, S. Mendioroz, and J. L. G. Fierro, Elsevier (2000), p. 157.
150 M. Anpo and M. Takeuchi, *Inter. J. Photoenergy.*, **3**, 1 (2001).
151 H. Yamashita and M. Anpo, *Catal. Surv. Asia*, **8**, 35 (2004), and references therein.
152 H. Yamashita, M. Harada, J. Misaka, M. Takeuchi, Y. Ichihashi, F. Goto, M. Ishida, T. Sasaki, and M. Anpo, *J. Synchrotron Rad.*, **8**, 569 (2001).
153 K. Takami, N. Segawa, H. Uehara, and M. Anpo, *Shokubai*, **41**, 295 (2002).
154 H. Yamashita, M. Harada, J. Misaka, M. Takeuchi, K. Ikeue, and M. Anpo, *J. Photochem. Photobiol., A*, **148**, 257 (2002).
155 M. Anpo and M. Takeuchi, *J. Catal.*, **216**, 505 (2003).
156 M. Anpo and M. Takeuchi, "Handbook of Ion Engineering," Institute of Ion-Engineering, Osaka (2002), p. 943.
157 M. Takeuchi, M. Anpo, T. Hirao, N. Itoh, and N. Iwamoto, *Surf. Sci. Jpn.*, **22**, 9, 561 (2001).

Masakazu Anpo born on 5 August 1946, completed his Ph.D from the Graduate School of Engineering, Osaka Prefecture University in 1975 and is presently a professor at the same university since 1990. His main research areas are (1) photochemistry of ketone molecules adsorbed on solid surfaces such as zeolites and within zeolite cavities (surface photochemistry); (2) photocatalysis of nano-sized TiO_2 powders; design and development of visible light-responsive TiO_2 photocatalysts in both powder and thin-film forms by applying ion-engineering techniques; (3) understanding the local structures and photoreactvities of various transition metal oxides such as Ti-, V-, Mo-, and Cr-oxide species as well as cations such as Cu(I) and Ag(I) which are highly dispersed within zeolite framework structures. He was offered many research associate positions at the National Research Council, Canada (NRC), Universite Pierre et Marie Curie in Paris (Paris 6th University), Torino University, East China University of Science and Technology (Shanghai), Tokyo Institute of Technology, Nagoya University, The University of Tokyo, Kyusyu University, etc., total of 21 universities. He was given the Japan Photochemistry Society Award in 1994; the 28th Mitsubishi Foundation in 1998; the Award of the Ueda Science Promotion in 2000; and the Chemical Society of Japan Award for Creative Work in 2002. He was invited to present the plenary lectures, keynote lectures, and invited lectures at many international congresses and conferences, total of 50 invited lectureship. He has published many books as an editor such as "Photochemistry on Solid Surfaces", (Elsevier), "Surface Photochemistry", (Wiley), and "Photofunctional Zeolites", (Nova Sciences), etc. His research works have been published in total of 514 publications including 322 original papers, 57 books, 78 reviews, and 57 proceedings. M. Anpo is the chief editor of the international journal, "Research on Chemical Intermediates", (VSP). He is a member of the editorial board of many journals such as Catal. Lett., Topics in Catal., Appl. Catal., Catal. Surveys from Asia, Current Opinion Solid State Materials Science, etc., total of 10 journals.